SIAM J. APPL. MATH.
Vol. 82, No. 3, pp. 773–792

ASYMPTOTIC ANALYSIS ON THE SHARP INTERFACE LIMIT OF THE TIME-FRACTIONAL CAHN–HILLIARD EQUATION*

TAO TANG†, BOYI WANG‡, AND JIANG YANG§

Abstract. In this paper, we aim to study the motions of interfaces and coarsening rates governed by the time-fractional Cahn–Hilliard equation (TFCHE). It is observed by many numerical experiments that the microstructure evolution described by the TFCHE displays quite different dynamical processes compared with the classical Cahn–Hilliard equation, in particular, regarding motions of interfaces and coarsening rates. By using the method of matched asymptotic expansions, we first derive the sharp interface limit models. Then we can theoretically analyze the motions of interfaces with respect to different timescales. For instance, for the TFCHE with the constant diffusion mobility, the sharp interface limit model is a fractional Stefan problem at the timescale $t = O(1)$. However, on the timescale $t = O(\varepsilon^{-\frac{1}{\alpha}})$, the sharp interface limit model is a fractional Mullins–Sekerka model. Similar asymptotic regime results are also obtained for the case with one-sided degenerated mobility. Moreover, the scaling invariant property of the sharp interface models suggests that the TFCHE with constant mobility preserves an $\alpha/3$ coarsening rate, and a crossover of the coarsening rates from $\frac{\alpha}{3}$ to $\frac{\alpha}{4}$ is obtained for the case with one-sided degenerated mobility, in good agreement with the numerical experiments.

Key words. method of matched asymptotic expansions, time-fractional Cahn–Hilliard equation, phase-field modeling, coarsening rates, motion of interfaces

AMS subject classifications. 65M30, 65M15, 65M12

DOI. 10.1137/21M1427863

1. Introduction.

The coarsening progcess (see Figure 1.1(a)–(c)) is a ubiquitous phenomenon and is observed in many fields, such as the study of solids or fluids in material science, opinion dynamics in social science, and pattern formation in biological science [10]. It is marked by an increase of the typical length scale in the spatial structures, which is due to the decrease of the interfacial energy [7, 11, 12, 13, 14, 22]. During the coarsening process, a power law, i.e., the increasing of a characteristic length scale with respect to the power of time, is often observed [11, 12, 34]; see also Figure 1.1(d). To measure the coarsening process, a coarsening rate is introduced. It is clear that the Cahn–Hilliard equation (CHE) can be used for simulating the coarsening progcess with an 1/3 power law. This power law coincides with the

*Received by the editors June 18, 2021; accepted for publication (in revised form) December 1, 2021; published electronically May 3, 2022.
https://doi.org/10.1137/21M1427863
Funding: This work was partially supported by the Special Project on High-Performance Computing of the National Key R&D Program (no. 2016YFB0200604), by the National Natural Science Foundation of China (NSFC) through grant no. 11731006, by the NSFC/Hong Kong RGC Joint Research Scheme (NSFC/RGC 11961160718), and by the fund of the Guangdong Provincial Key Laboratory of Computational Science and Material Design (no. 2019B030301001). The work of the third author was supported by the National Science Foundation of China (NSFC-11871264).

†Division of Science and Technology, BNU-HKBU United International College, Zhuhai, Guangdong, People's Republic of China, and SUSTech International Center for Mathematics, Southern University of Science and Technology, Shenzhen 518055, People's Republic of China (tangt@sustech.edu.cn).

‡Department of Mathematics, Southern University of Science and Technology, Shenzhen 518055, People's Republic of China, and Department of Mathematics, National University of Singapore, 119076 Singapore (11755001@mail.sustech.edu.cn).

§Department of Mathematics and SUSTech International Center for Mathematics, Southern University of Science and Technology, Shenzhen 518055, People's Republic of China (yangj7@sustech.edu.cn).

coarsening rate indicated by the classical Lifshitz–Slyozov–Wagner theory for bulk diffusion. However, different coarsening rates have also been discovered, which suggests that the CHE is insufficient. For example, significantly small coarsening rates, i.e., 0.13, 0.07, and 0.09, are observed in the coarsening of γ' precipitates [19, 32]. The authors explain that as a result of the existence of the elastic strain field. In addition, a coarsening rate of $1/2$ is observed in the study of precipitate in rapidly solidified Al-Si alloy, and it is due to a change of the annealing temperature according to the author [7]. More examples of different coarsening process are introduced in [10]. These results suggest that the CHE may not be a suitable coarsening model of every case, and other models should be considered.

Recently, time-fractional models have drawn people's attention [2, 8, 16, 17, 20, 25, 26, 23, 37, 24]. Numerical results have shown that the coarsening rate of a time-fractional Cahn–Hilliard equation (TFCHE) depends not only on the mobility but also on the order of the fractional derivative [24, 27, 30, 34, 38, 17]. Especially, an intriguing coarsening rate of $\alpha/3$ is observed in [34]. Figure 1.1(a)–(d) shows the case for $\alpha = 0.9$.

This paper is concerned with the motion of interfaces and coarsening dynamics of the TFCHE

$$\begin{cases} \partial_t^\alpha u = \nabla(M(u)\nabla\mu), \\ \mu = -\varepsilon^2\Delta u + F'(u), \quad x \in \Omega, \quad 0 < t < T, \end{cases} \tag{1.1}$$

where, for some given $0 < \alpha < 1$, ∂_t^α is the Caputo fractional derivative [2, 21, 31] defined by

$$\partial_t^\alpha u = \frac{1}{\Gamma(1-\alpha)} \int_0^t \frac{u'(\tau)}{(t-\tau)^\alpha} d\tau, \quad t > 0.$$

As a nonlocal-in-time extension of classical phase-field models, u is the order parameter, ε represents the width of interfaces, and μ is the chemical potential. Without loss of generality, we restrict our attention to the commonly used double well potential

$$F(u) = \frac{1}{4}(u^2 - 1)^2. \tag{1.2}$$

In (1.1), the diffusion mobility function $M(u)$ is taken as the constant 1 or the one-sided degenerate function $1 + u$. For simplicity, (1.1) is subject to the Neumann boundary conditions

$$\frac{\partial u}{\partial n} = \frac{\partial \mu}{\partial n} = 0, \quad x \in \partial\Omega, \quad 0 < t < T, \tag{1.3}$$

and the initial data

$$u(x, 0) = u_0(x), \quad x \in \Omega. \tag{1.4}$$

Extensive investigations have been made to study the coarsening process and the coarsening rates of the CHE. Pego [28] studied the asymptotic regimes on CHE with the constant mobility by the method of matched asymptotic expansions. Alikakos, Bates, and Chen [1] proved the convergence of CHE to the Mullins–Sekerka (MS) equations. Cahn, Elliott, and Novick-Cohen [6] studied the degenerate CHE and obtained the surface diffusion model. In addition, it has been shown that the coarsening rate of the CHE is related to the diffusion mobility. Dai and Du [11, 12] studied the motion of interfaces for CHE with single-sided degenerate mobility, and they obtained its sharp

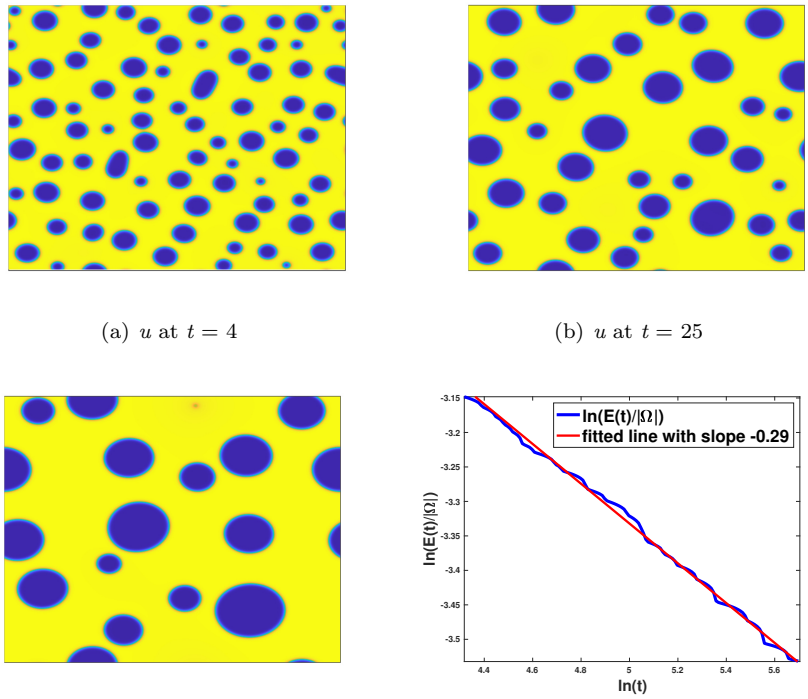

(a) u at $t = 4$ (b) u at $t = 25$

(c) u at $t = 100$ (d) evolution of energy

FIG. 1.1. $M(u) = 1$, $\alpha = 0.9$, $\varepsilon = 0.05$. *Morphological patterns at* $t = 4$ *(top left),* $t = 25$ *(top right),* $t = 100$ *(bottom left),* $\ln(E(t)/|\Omega|)$ *vs.* $\ln(t)$ *(bottom right).*

interface limits as well as the coarsening rates. Moreover, Chen et al. presented a careful numerical study for a thin film model without slope selection [9], with particular attention to the energy coarsening dependence on the interface width parameter. More results related to the CHE can be found in, i.e., [1, 3, 4, 13, 15, 33, 36, 14, 35].

Motivated by the above asymptotic analysis theory and numerical results on the coarsening rates for time-fractional CHE, we will establish asymptotic regime theory on the TFCHE by the method of matched asymptotic expansion as used in [28] and to derive the surface diffusion models of interface motion for the TFCHE. As far as we know, this is the first work to study the coarsening process and coarsening rate of TFCHEs using formal asymptotic matching.

Our main results are twofold. First, a formal asymptotic description of the TFCHE in the later regime of phase separation is given, where different types of mobilities are discussed. Second, using the resulting sharp interface models and the scaling invariant property, we explain the corresponding coarsening rates for the TFCHEs, which agrees well with numerical observations in [34, 38]. A more precise outline of the first result is given below. In a slow timescale $O(1)$, the solution at leading order satisfies a nonlocal "Stefan problem" with equilibrium condition at the interface, and the leading order inner solution is the solution to the problem

$$F'(U) - \partial_{zz}U = 0, \tag{1.5a}$$

$$U(-\infty) = -1, \qquad U(+\infty) = 1, \quad U(0) = 0, \tag{1.5b}$$

which is the rescaled tanh function $U(z) = \tanh(z/\sqrt{2})$. Then, on a much more slower timescale $t_1 = \varepsilon^{\frac{1}{\alpha}} t$, phase equilibrium holds everywhere, and interface motion is governed by μ_1, which is the second term in the asymptotic expansion of the chemical potential μ, obeying the following nonlocal MS model:

$$\partial_{t_1}^{\alpha} u_0 = \Delta \mu_1 \qquad \text{in } \Omega \backslash \Gamma, \tag{1.6a}$$

$$\mu_1 = \kappa \frac{S}{[U]} \qquad \text{on } \Gamma, \tag{1.6b}$$

$$\mathrm{I}^{1-\alpha} V = [\partial_{\mathbf{m}} \mu]_{-}^{+} / [U] \qquad \text{on } \Gamma. \tag{1.6c}$$

In (1.6a)–(1.6c), S and $[U]$ are some constants, u_0 is the sign function of the distance function ϕ, Γ is the interface, $\kappa = \Delta\phi$ is the mean curvature, $V = \partial_t \phi$ is the normal velocity of Γ on x with the signed distance ϕ from the point $x \in \Omega$ to interface, $\mathbf{m}$ is the unit normal vector on Γ, $\mathrm{I}^{1-\alpha}$ denotes the fractional integral operator, and u_0 is determined by the interface Γ and equals ± 1 in $\Omega^{\pm}$, correspondingly. The present results reduce to the classical one of Pego [28] for local CHE,

$$V = [\partial_{\mathbf{m}} \mu_1]_{-}^{+} / [U], \qquad \text{on } \Gamma,$$

by letting $\alpha \to 1$.

As for the case with one-sided degenerate mobility, i.e., $M(u) = 1 + u$, the corresponding sharp interface models in timescales $t_1 = \varepsilon^{\frac{1}{\alpha}} t$ and $t_2 = \varepsilon^{\frac{2}{\alpha}} t$ are derived, respectively, as the following nonlocal MS models:

$$\partial_{t_1}^{\alpha} u_0 = \Delta \mu_1 \qquad \text{in } \Omega^{+}, \tag{1.7a}$$

$$\mu_1 = -\kappa \frac{S}{[U]} \qquad \text{on } \Gamma, \tag{1.7b}$$

$$\mathrm{I}^{1-\alpha} V = \partial_{\mathbf{m}} \mu_1^{+} \qquad \text{on } \Gamma \tag{1.7c}$$

and

$$\partial_{t_2}^{\alpha} u_0 = \nabla(\mu_1 \nabla \mu_1) \qquad \text{in } \Omega^{-}, \tag{1.8a}$$

$$\mu_1 = -\kappa \frac{S}{[U]} \qquad \text{on } \Gamma, \tag{1.8b}$$

$$2\Delta \mu_2 = \partial_t^{\alpha} u_0 \qquad \text{in } \Omega^{+}, \tag{1.8c}$$

$$\mu_2 = -\kappa^2 \frac{S_1}{[U]} \qquad \text{on } \Gamma, \tag{1.8d}$$

$$\mathrm{I}^{1-\alpha} V = \partial_{\mathbf{m}} \mu_2^{+} + \frac{1}{4} \mu_1^{-} \partial_{\mathbf{m}} \mu_1^{-} \qquad \text{on } \Gamma. \tag{1.8e}$$

A more precise outline of the second model is given below. For the case with the constant mobility $M(u) = 1$, the scaling invariant of the nonlocal MS model implies a coarsening rate of $\alpha/3$, which coincides well with that observed in numerical experiments. For the case with one-sided degenerate mobility $M(u) = 1 + u$, the models (1.7a)–(1.7c) and (1.8a)–(1.8e) exhibit two different coarsening rates of $\frac{\alpha}{3}$ and $\frac{\alpha}{4}$, respectively, which are in good agreement with the observations in [11, 12].

The rest of the paper is organized as follows. In sections 2 and 3, we establish sharp interface limit models for the TFCH system (1.1)–(1.4) when $M(u) = 1$ and $M(u) = 1 + u$, respectively. In section 4, the scaling invariant properties of sharp interface models and the coarsening rates will be discussed. Some concluding remarks are given in the final section.

2. Sharp interface models when $M(u) = 1$. The method of matched asymptotic expansions expansion as in Pego [28] will be used in this section. For all $\gamma \in \mathbb{R}$ and $t_1 = \varepsilon^\gamma t$, simple calculation yields

$$\partial_t^\alpha v(t_1) = \frac{\varepsilon^{\alpha\gamma}}{\Gamma(1-\alpha)} \int_0^{\varepsilon^\gamma t} \frac{v'(\tau)}{(\varepsilon^\gamma t - \tau)^\alpha} d\tau = \varepsilon^{\alpha\gamma} \partial_{t_1}^\alpha v(t_1). \tag{2.1}$$

Below we will develop sharp interface models at different timescales. We assume that with domain $\Omega \subset \mathbb{R}^N$, $N = 2$ or 3, there is a smooth $N-1$ dimension interface Γ which divides Ω into Ω^+ and Ω^-. For simplifying the problem, we assume the interface Γ does not intersect with the boundary. Such an assumption is made to avoid the analysis on boundary layers involved by the intersection. We point out that the asymptotic analysis involving boundary layers for the regular CHE has been presented by Dziwinik, Münch, and Wagner [18].

2.1. The timescale $t = O(1)$: A time-fractional Stefan problem. We assume that the phase structures are nearly equilibrated.

2.1.1. Outer expansion. We expand the solution in a series of powers of ε in the timescale t:

$$u(x,t) = u_0(x,t) + \varepsilon u_1(x,t) + \cdots, \tag{2.2a}$$

$$\mu(x,t) = \mu_0(x,t) + \varepsilon \mu_1(x,t) + \cdots. \tag{2.2b}$$

In this timescale,

$$\partial_t^\alpha u = \partial_t^\alpha u_0 + \varepsilon \partial_t^\alpha u_1 + \cdots. \tag{2.3}$$

By comparing (2.3) with (1.1) and matching the powers of ε, we get

$$\partial_t^\alpha u_0 = \Delta \mu_0, \quad \mu_0 = F'(u_0). \tag{2.4}$$

This method will be used many times in this paper. The leading order equation implies that the phase parameters evolve according to the chemical potential. The boundary condition on $\partial\Omega$ is taken naturally as $\frac{\partial u_0}{\partial n} = 0$. To model this problem, it is necessary to derive the boundary conditions on the interface, which can be done by matching outer solutions with the inner solutions.

2.1.2. Inner expansion. Now we consider the inner expansions near the front. Intuitively, the inner solutions take the value of the solutions restricted on the interface. The inner solutions will be defined in this region by an inner variable z. Moreover, the inner solution matches with the outer solution when $z \to \pm\infty$ according to some specified matching conditions. We take the same notations as Pego [28]. In order to define the inner variable z, define the stretched normal distance to the front

$$z = \phi(x,t)/\varepsilon,$$

where $\phi(x,t)$ is the signed distance of the point x in Ω to the interface $\Gamma(t)$ such that $\phi > 0$ in Ω^+ and $\phi < 0$ in Ω^-. Note that ϕ is a smooth function near Γ if Γ is smooth.

Consider the functions $\tilde{v} = \tilde{v}(z,x,t)$ defined near the interface. Following [28], we require that v does not vary when x varies normally to Γ but z holds, that is, $\tilde{v}(z, x + \alpha\nabla\phi, t) = \tilde{v}(z, x + \nabla\phi, t)$ for small α or $\nabla\phi \cdot \nabla_x \tilde{v} = 0$. Moreover, define

$$\boldsymbol{m} = \nabla\phi(x,t), \quad \kappa = \Delta\phi(x,t), \quad V(x,t) = \partial_t \phi(x,t), \tag{2.5}$$

where $\boldsymbol{m}$ is the unit normal vector on Γ pointing toward Ω^+, κ is the mean curvature of Γ at point x, and $\partial_t\phi = V(x,t)$ is the normal velocity of front motion in this timescale, which is positive when pointing toward Ω^-. We also assume that $\partial_t\phi = V(x,t)$ exists for all $x \in \Omega$. Given $\tilde{v}(z,x,t)$ and $v = \tilde{v}(\phi(x,t)/\varepsilon, x, t)$, we have derivatives transform according to the relations [28]

$$\nabla v = \nabla_x \tilde{v} + \varepsilon^{-1}\mathbf{m}\partial_z \tilde{v}, \tag{2.6a}$$

$$\Delta v = \Delta_x \tilde{v} + \varepsilon^{-1}\kappa\partial_z \tilde{v} + \varepsilon^{-2}\partial_{zz}\tilde{v}, \tag{2.6b}$$

$$\partial_t v = \varepsilon^{-1}\partial_t\phi\partial_z\tilde{v} + \partial_t\tilde{v}. \tag{2.6c}$$

For the inner expansion, we have

$$u(x,t) = \tilde{u}_0(z,x,t) + \varepsilon\tilde{u}_1(z,x,t) + \cdots, \tag{2.7a}$$

$$\mu(x,t) = \tilde{\mu}_0(z,x,t) + \varepsilon\tilde{\mu}_1(z,x,t) + \cdots. \tag{2.7b}$$

By Taylor expansion and (2.7a)–(2.7b), the expansions are related by

$$\tilde{\mu}_0 = F'(\tilde{u}_0) - \partial_{zz}\tilde{u_0}, \tag{2.8a}$$

$$\tilde{\mu}_1 = F''(\tilde{u}_0)\tilde{u}_1 - \partial_{zz}\tilde{u}_1 - \kappa\partial_z\tilde{u}_0, \tag{2.8b}$$

$$\tilde{\mu}_2 = F''(\tilde{u}_0)\tilde{u}_2 - \partial_{zz}\tilde{u}_2 - \kappa\partial z\tilde{u}_1 + \frac{1}{2}F'''(\tilde{u}_0)\tilde{u}_1^2 - \Delta_x\tilde{u}_0. \tag{2.8c}$$

Substituting the expansion back to (1.1), using the derivative transform formulas (2.6a)–(2.6c), and matching the lowest-order term of ε shows.

$$\partial_{zz}\tilde{\mu}_0 = 0. \tag{2.9}$$

Integrating (2.9) and combining (2.8a), we derive

$$\tilde{\mu}_0 = a_0(x,t)z + b_0(x,t) = F'(\tilde{u}_0) - \partial_{zz}\tilde{u}_0. \tag{2.10}$$

Since $\tilde{u}_0$ must be bounded, $a_0(x,t)$ has to be zero. Then we derive b_0 by solving the following system:

$$F'(\tilde{u}_0) - \partial_{zz}\tilde{u}_0 = b_0, \tag{2.11a}$$

$$\tilde{u}_0(+\infty,x,t) = u^+(x,t), \quad \tilde{u}_0(-\infty,x,t) = u^-(x,t). \tag{2.11b}$$

Letting $z \to \pm\infty$ in (2.11a) and integrating (2.11a) with respect to u yields

$$F'(u^+(x,t)) = F'(u^-(x,t)) = b_0(x,t), \tag{2.12a}$$

$$b_0(x,t)(u^+(x,t) - u^-(x,t)) = F(u^+(x,t)) - F(u^-(x,t)). \tag{2.12b}$$

Assuming that the leading order inner solution u_0 links the two pure phases ± 1 means

$$u^+(x,t) = 1, \quad u^-(x,t) = -1. \tag{2.13}$$

Therefore,

$$b_0 = \tilde{\mu}_0(z) = 0. \tag{2.14}$$

Recall (2.11a) with $b_0 = 0$. As in [11], we choose the well-known solution profile

$$\tilde{u}_0(z) = \tanh\left(\frac{z}{\sqrt{2}}\right) =: U(z). \tag{2.15}$$

Matching with the outer solution by (2.4) derives the boundary conditions for the equilibrium state

$$\mu_0 = 0 \quad \text{on} \quad \Gamma. \tag{2.16}$$

For the matching between higher-order terms, we follow the ideas provided by Caginalp and Fife in [5]. Fixing x on Γ, we seek to match the expansions by requiring formally that

$$(\mu_0 + \varepsilon\mu_1 + \cdots)|_{(x+\varepsilon z\boldsymbol{m},t)} \approx (\tilde{\mu}_0 + \varepsilon\tilde{\mu}_1 + \cdots)|_{(z,x,t)} \tag{2.17}$$

when εz is between $o(1)$ and $O(\varepsilon)$. Expanding the left-hand side in powers of ε as $\varepsilon z \to 0+$ gives

$$\mu_0^+ + \varepsilon(\mu_1^+ + zD_m\mu_0^+) + \varepsilon^2(\mu_2^+ + zD_m\mu_1^+ + \frac{1}{2}z^2D_m^2\mu_0^+) + \cdots, \tag{2.18}$$

where D_m denotes the directional derivative along $\boldsymbol{m}$ and μ_i^+ is the limit when $z \to 0$ along $\boldsymbol{m}$:

$$\mu_i^{\pm} = \lim_{z\to 0^{\pm}} \mu_i(x + z\boldsymbol{m}, t_1). \tag{2.19}$$

Similar results hold for $\varepsilon z \to 0^-$. To match these expansions in (2.18) with the inner expansion, one requires

$$\mu_0^{\pm}(x,t) = \tilde{\mu}_0(z,x,t), \qquad z \to \pm\infty, \tag{2.20a}$$

$$(\mu_1^{\pm} + zD_m\mu_0^{\pm})(x,t) = \tilde{\mu}_1(z,x,t), \qquad z \to \pm\infty, \tag{2.20b}$$

$$(\mu_2^+ + zD_m\mu_1^+ + \frac{1}{2}z^2D_m^2\mu_0^+)(x,t) = \tilde{\mu}_2(z,x,t), \qquad z \to \pm\infty. \tag{2.20c}$$

The time derivative in the local frame equals

$$\begin{aligned}
&\partial_t^\alpha u(x,t) = \partial_t^\alpha\left((\tilde{u}_0 + \varepsilon\tilde{u}_1 + \cdots)|_{(\phi(x,t)/\varepsilon,x,t)}\right)\\
=&\frac{1}{\Gamma(1-\alpha)}\int_0^t \frac{\varepsilon^{-1}\partial_\tau\phi(x,\tau)\partial_z\tilde{u}_0(\phi(x,\tau)/\varepsilon)}{(t-\tau)^\alpha}d\tau\\
&+\frac{1}{\Gamma(1-\alpha)}\int_0^t \frac{\partial_\tau\phi(x,\tau)\partial_z\tilde{u}_1(\phi(x,\tau)/\varepsilon,x,\tau) + \varepsilon(\partial_\tau\tilde{u}_1(z,x,\tau)|_{z=\phi(x,\tau)/\varepsilon})}{(t-\tau)^\alpha}d\tau + \cdots\\
=&\frac{1}{\Gamma(1-\alpha)}\int_0^t \frac{\varepsilon^{-1}\partial_\tau\phi(x,\tau)\partial_z\tilde{u}_0(\phi(x,\tau)/\varepsilon,x,\tau)}{(t-\tau)^\alpha}d\tau + h.o.t.
\end{aligned} \tag{2.21}$$

Then matching the $O(\frac{1}{\varepsilon})$ term gives

$$\frac{1}{\Gamma(1-\alpha)}\int_0^t \frac{\partial_\tau\phi(x,\tau)\partial_z\tilde{u}_0(\phi(x,\tau)/\varepsilon)}{(t-\tau)^\alpha}d\tau = \tilde{\mu}_{1zz}(z,x,t). \tag{2.22}$$

Integrating (2.22) with respect to z over $(-\infty, +\infty)$, we get

$$\frac{1}{\Gamma(1-\alpha)} \int_0^t \frac{\phi_\tau(x,\tau)}{(t-\tau)^\alpha} d\tau U\big|_{-\infty}^{+\infty} = \tilde{\mu}_{1z}\big|_{-\infty}^{+\infty}. \tag{2.23}$$

By using the matching condition (2.20b), we derive

$$\frac{1}{\Gamma(1-\alpha)} \int_0^t \frac{\phi_\tau(x,\tau)}{(t-\tau)^\alpha} d\tau = [\mathbf{m}\cdot\nabla\mu_0]_-^+ [U]^{-1}, \tag{2.24}$$

where $[U] = U\big|_{-\infty}^{+\infty} = 2$ and $[\mathbf{m}\cdot\nabla\mu_0]_-^+$ denotes the jump of the direction derivative of μ over the interface along the normal vector. We rewrite (2.24) in the following form using the notation of fractional integral:

$$\mathrm{I}^{1-\alpha} V = \frac{1}{2}[\partial_{\mathbf{m}}\mu_0]_-^+. \tag{2.25}$$

Sharp interface model in $t = O(1)$. Ignoring the subscripts, the sharp interface model is a time-fractional Stefan model:

$$\partial_t^\alpha u_0 = \Delta\mu_0,\ \mu_0 = F'(u_0), \qquad \text{in } \Omega/\Gamma, \tag{2.26a}$$

$$u_0 = 1 \text{ on } \Gamma^+, \quad u_0 = -1 \text{ on } \Gamma^-, \tag{2.26b}$$

$$\mu_0 = 0 \qquad \text{on } \Gamma, \tag{2.26c}$$

$$\mathrm{I}^{1-\alpha} V = \frac{1}{2}[\partial_{\mathbf{m}}\mu_0]_-^+. \tag{2.26d}$$

2.2. The timescale $t_1 = \varepsilon^{\frac{1}{\alpha}} t$: A time-fractional MS model. In this part we derive the time-fractional sharp interface model in the timescale $t_1 = \varepsilon^{\frac{1}{\alpha}} t$.

2.2.1. Outer expansion. In this timescale,

$$\partial_t^\alpha u = \varepsilon \partial_{t_1}^\alpha u_0 + \varepsilon^2 \partial_{t_1}^\alpha u_1 + \cdots. \tag{2.27}$$

Similar to (2.4), we have

$$0 = \Delta\mu_0, \quad \mu_0 = F'(u_0), \quad \partial_{t_1}^\alpha u_0 = \Delta\mu_1, \quad \partial_{t_1}^\alpha u_1 = \Delta\mu_2. \tag{2.28}$$

In this timescale, at leading order, we have a steady-state equation for μ_0. In order to establish the limit model, we also need the boundary conditions on the boundary $\partial\Omega$ and the interface Γ. The boundary condition on $\partial\Omega$ is naturally inherited from the boundary condition $\frac{\partial u}{\partial n} = 0$, but for the boundary conditions on the interface, we need to solve for them by asymptotically matching the outer solutions and the inner solutions.

2.2.2. Inner expansion. Similar to (2.9), matching $1/\varepsilon^2$ and $1/\varepsilon$ terms in the second equation in (1.1) yields

$$\partial_{zz}\tilde{\mu}_0 = 0, \tag{2.29a}$$

$$\kappa\partial_z\tilde{\mu}_0 + \partial_{zz}\tilde{\mu}_1 = 0. \tag{2.29b}$$

Analogous analysis to section 2.1 leads to a tanh profile again, i.e.,

$$\tilde{u}_0 = U(z), \quad \tilde{\mu}_0 = 0,$$

where $U(z)$ is defined in (2.15). We also assume that $u_0^+(x,t_1)=1, \quad u_0^-(x,t_1)=-1$. Matching the inner solution with the outer solution according to (2.20a), one derives the boundary conditions for the outer solution

$$\mu_0 = 0 \quad \text{on } \Gamma. \tag{2.30}$$

Notice that now $\Delta\mu_0 = 0$ and $\mu_0 = F'(u_0)$ in (2.28); therefore,

$$\mu_0 = 0 \quad \text{in} \quad \Omega, \quad u_0 \equiv -1 \quad \text{in} \quad \Omega^-, \quad \text{and} \quad u_0 \equiv 1 \quad \text{in} \quad \Omega^+.$$

As for $\tilde{\mu}_1$, we have

$$\tilde{\mu}_1 = F''(\tilde{u}_0)\tilde{u}_1 - \partial_{zz}\tilde{u}_1 - \kappa\partial_z\tilde{u}_0 = b_2(x,t_1). \tag{2.31}$$

Since $F''(\tilde{u}_0)\tilde{u}_0'(z) - \partial_{zz}\tilde{u}_0' = 0$, multiplying (2.31) by U' and integrating by z on $(-\infty,+\infty)$ yields

$$[U]\tilde{\mu}_1 + \kappa S = 0,$$

where

$$S = \int_{-\infty}^{+\infty} U'(z)^2 dz, \quad [U] = u^+ - u^- = 2.$$

Using the matching conditions (2.20b),

$$\mu_1 = \tilde{\mu}_1 = -\kappa\frac{S}{[U]} \quad \text{on } \Gamma.$$

Letting $\varepsilon \to 0$, we have the boundary conditions of μ at the interface Γ. Therefore, we have a closed system for μ_1,

$$\partial_{t_1}^{\alpha} u_0 = \Delta\mu_1 \qquad \text{in } \Omega\backslash\Gamma, \tag{2.32a}$$

$$\mu_1 = -\kappa\frac{S}{[U]} \qquad \text{on } \Gamma, \tag{2.32b}$$

$$\partial_{\mathbf{m}}\mu_1 = 0 \qquad \text{on } \partial\Omega, \tag{2.32c}$$

provided that Γ is known and smooth, which is well-defined and can be solved independently in each $\Omega^{\pm}$.

Similar to (2.24), in this new timescale, we have

$$\frac{1}{\Gamma(1-\alpha)}\int_0^{t_1}\frac{\phi_\tau(x,\tau)}{(t_1-\tau)^{\alpha}}d\tau = [\mathbf{m}\cdot\nabla\mu_1]_-^+[U]^{-1}, \tag{2.33}$$

which is

$$\mathrm{I}^{1-\alpha}V = \frac{1}{2}[\partial_{\mathbf{m}}\mu_1]_-^+. \tag{2.34}$$

Sharp interface model in $t_1 = \varepsilon^{\frac{1}{\alpha}}t$. Collecting the above equations (2.32a)–(2.32c), we get the sharp interface model as follows:

$$\partial_{t_1}^{\alpha} u_0 = \Delta\mu_1 \qquad \text{in } \Omega\backslash\Gamma, \tag{2.35a}$$

$$\mu_1 = -\kappa\frac{S}{[U]} \qquad \text{on } \Gamma, \tag{2.35b}$$

$$\frac{\partial\mu_1}{\partial n} = 0 \qquad \text{on } \partial\Omega, \tag{2.35c}$$

$$\mathrm{I}^{1-\alpha}V = \frac{1}{2}[\partial_{\mathbf{m}}\mu_1]_-^+ \qquad \text{on } \Gamma. \tag{2.35d}$$

$u_0 \equiv 1$ or $u_0 \equiv 1$ when $\phi > 0$ or $\phi < 0$, respectively. The system (2.35a)–(2.35d) is well-posed, which determines the motion of the front for given smooth initial data. It is a time-fractional MS model.

REMARK 1. Since u_0 is the sign function of ϕ, $\partial_t u_0 \equiv 0$. Hence, in the local CH model, (2.35a) becomes

$$\Delta \mu_1 = 0 \quad \text{in } \Omega \backslash \Gamma.$$

But for the TFCHE, it is necessary to keep $\partial_{t_0}^{\alpha} u_0$ due to the nonlocal effect.

3. Sharp interface models when $M(u) = 1+u$. In this section, we intend to derive the sharp interface models of the TFCHE with one-sided mobility $M(u) = 1+u$ under the same problem setting as in section 2. To begin with, special treatments are required for the degenerate mobility since in this case the leading order term $1+u_0$ in the asymptotic expansion of $M(u)$ might not be valid when $z \to -\infty$. Assuming that $1+\tilde{u}_0$ decreases exponentially, that is, $1+\tilde{u}_0 \sim e^{z/\sigma}, z \to -\infty$. Taking $\eta = \sigma \ln \frac{1}{\varepsilon}$, we have the following estimates of $1+\tilde{u}_0$:

$$1+\tilde{u}_0 = \begin{cases} O(\varepsilon) & \text{if} \quad z \le -\eta, \\ O(\varepsilon^2) & \text{if} \quad z \le -2\eta, \\ O(\varepsilon^3) & \text{if} \quad z \le -3\eta, \\ O(\varepsilon^4) & \text{if} \quad z \le -4\eta. \end{cases} \tag{3.1}$$

To simplify the notations, we denote $\chi_4 = 1_{(-\infty,-4\eta]}$, $\chi_3 = 1_{(-4\eta,-3\eta]}$, $\chi_2 = 1_{(-3\eta,2\eta]}$, $\chi_1 = 1_{(-2\eta,\eta]}$, and $\chi_0 = 1_{(-\eta,+\infty)}$, which are the corresponding characteristic functions on each interval. Then we have the following expansion of $1+\tilde{u}_0$:

$$\begin{aligned} &1+\tilde{u}_0 \\ &= (1+\tilde{u}_0)\chi_0 + \varepsilon(1+\tilde{u}_0)\varepsilon^{-1}\chi_1 + \varepsilon^2(1+\tilde{u}_0)\varepsilon^{-2}\chi_2 + \varepsilon^3(1+\tilde{u}_0)\varepsilon^{-3}\chi_3 + \varepsilon^4(1+\tilde{u}_0)\varepsilon^{-4}\chi_4. \end{aligned} \tag{3.2}$$

Replacing $1+\tilde{u}_0$ by the above expansion gives a valid series of $M(u)$. Moreover, a similar idea is applied for $\tilde{u}_{0z}$. When $z \to -\infty$, $\tilde{u}_{0z}$ decays at the same rate as $1+\tilde{u}_0$. As for when $z \to +\infty$, we assume that $\tilde{u}_{0z} \sim e^{-z/\hat{\sigma}}$ and $\hat{\eta} = \hat{\sigma} \ln \frac{1}{\varepsilon}$, so $\tilde{u}_{0z} \le O(\varepsilon)$ when $z \ge \hat{\eta}$. Let the partitions be $[-\eta, \hat{\eta})$, $[-2\eta, -\eta) \cup [\hat{\eta}, 2\hat{\eta})$, $[-3\eta, -2\eta) \cup [2\hat{\eta}, 3\hat{\eta})$, $[-4\eta, -3\eta) \cup [3\hat{\eta}, 4\hat{\eta})$, and $(-\infty, -4\eta) \cup [4\hat{\eta}, +\infty)$ and the corresponding characteristic functions be $\hat{\chi}_0, \hat{\chi}_1, \hat{\chi}_2, \hat{\chi}_3, \hat{\chi}_4$. Then the following expansion holds:

$$\tilde{u}_{0z} = \tilde{u}_{0z}\hat{\chi}_0 + \varepsilon\tilde{u}_{0z}\varepsilon^{-1}\hat{\chi}_1 + \varepsilon^2\tilde{u}_{0z}\varepsilon^{-2}\hat{\chi}_2 + \varepsilon^3\tilde{u}_{0z}\varepsilon^{-3}\hat{\chi}_3 + \varepsilon^4\tilde{u}_{0z}\varepsilon^{-4}\hat{\chi}_4. \tag{3.3}$$

With the above expansions, we can now compute $\nabla \cdot (M(u)\nabla\mu)$ as follows:

$$\nabla \cdot (M(u)\nabla\mu) = M'(u)\nabla_x u \cdot \nabla_x \mu + \varepsilon^{-2}\partial_z u \partial_z \mu + M(u)(\Delta_x \mu + \varepsilon^{-1}\kappa\partial_z \mu + \varepsilon^{-2}\partial_{zz}\mu). \tag{3.4}$$

By simple calculations, we find the terms of powers of ε in (3.4) correspondingly. The first four leading order terms are required in our later analysis, which are the $O(\frac{1}{\varepsilon^2})$ term

$$\hat{\chi}_0\tilde{u}_{0z}\tilde{\mu}_{0z} + \chi_0(1+\tilde{u}_0)\partial_{zz}\tilde{\mu}_0, \tag{3.5}$$

the $O(\frac{1}{\varepsilon})$ term

$$(\tilde{u}_{0z}\hat{\chi}_1\varepsilon^{-1}+\tilde{u}_{1z})\tilde{\mu}_{0z}+\tilde{u}_{0z}\hat{\chi}_0\tilde{\mu}_{1z}+\chi_0\kappa(1+\tilde{u}_0)\tilde{\mu}_{0z}+\chi_0(1+\tilde{u}_0)\tilde{\mu}_{1zz} \\ +(\tilde{u}_1+\chi_1(1+\tilde{u}_0)\varepsilon^{-1})\tilde{\mu}_{0zz}, \tag{3.6}$$

the $O(1)$ term

$$\nabla_x\tilde{u}_0\nabla_x\tilde{\mu}_0+(\hat{\chi}_0\tilde{u}_{0z}\tilde{\mu}_{2z}+(\hat{\chi}_1\tilde{u}_{0z}\varepsilon^{-1}+\tilde{u}_{1z})\tilde{\mu}_{1z}+(\hat{\chi}_2\tilde{u}_{0z}\varepsilon^{-2}+\tilde{u}_{2z})\tilde{\mu}_{0z}) \\ +\chi_0(1+\tilde{u}_0)(\Delta_x\tilde{\mu}_0+\kappa\tilde{\mu}_{1z}+\tilde{\mu}_{2zz})+(\varepsilon^{-1}(1+\tilde{u}_0)\chi_1+\tilde{u}_1)(\kappa\tilde{\mu}_{0z}+\tilde{\mu}_{1zz}) \\ +(\varepsilon^{-2}(1+\tilde{u}_0)\chi_2+\tilde{u}_2)\tilde{\mu}_{0zz}, \tag{3.7}$$

and the $O(\varepsilon)$ term

$$\nabla_x\tilde{u}_0\nabla_x\tilde{\mu}_1+\nabla_x\tilde{u}_1\nabla_x\tilde{\mu}_0+(\hat{\chi}_0\tilde{u}_{0z}\tilde{\mu}_{3z}+(\hat{\chi}_1\tilde{u}_{0z}\varepsilon^{-1}+\tilde{u}_{1z})\tilde{\mu}_{2z} \\ +(\hat{\chi}_2\tilde{u}_{0z}\varepsilon^{-2}+\tilde{u}_{2z})\tilde{\mu}_{1z}+(\hat{\chi}_3\tilde{u}_{0z}\varepsilon^{-3}+\tilde{u}_{3z})\tilde{\mu}_{0z})+ \\ +\chi_0(1+\tilde{u}_0)(\Delta_x\tilde{\mu}_1+\kappa\tilde{\mu}_{2z}+\tilde{\mu}_{3zz}) \\ +((1+\tilde{u}_0)\chi_1\varepsilon^{-1}+\tilde{u}_1)(\Delta_x\tilde{\mu}_0+\kappa\tilde{\mu}_{0z}+\tilde{\mu}_{2zz}) \\ +((1+\tilde{u}_0)\chi_2\varepsilon^{-2}+\tilde{u}_2)(\kappa\tilde{\mu}_{0z}+\tilde{\mu}_{1zz})+((1+\tilde{u}_0)\chi_3\varepsilon^{-3}+\tilde{u}_3)\tilde{\mu}_{0zz}. \tag{3.8}$$

We start with a nontrivial timescale in this section.

3.1. The timescale $t = O(1)$: A one-sided time-fractional Stefan problem.

3.1.1. Outer expansion. Similar to (2.28), it yields

$$\partial_t^\alpha u_0=\nabla((1+u_0)\nabla\mu_0),\quad \partial_t^\alpha u_1=\nabla((1+u_0)\nabla\mu_1+u_1\nabla\mu_0). \tag{3.9}$$

3.1.2. Inner expansion. In the same way as (2.29a)–(2.29b), the $O(\varepsilon^{-2})$ equation is

$$0=\hat{\chi}_0\tilde{u}_{0z}\tilde{\mu}_{0z}+\chi_0(1+\tilde{u}_0)\tilde{\mu}_{0zz}. \tag{3.10}$$

We rewrite (3.10) in the following form:

$$\chi_0\partial_z((1+\tilde{u}_0)\tilde{\mu}_{0z})+\hat{\chi}_0(1+\tilde{u}_0)\tilde{\mu}_{0zz}=0. \tag{3.11}$$

That is, for $z\in(-\eta,\hat{\eta})$,

$$\tilde{\mu}_{0zz}(1+\tilde{u}_0)+\tilde{\mu}_{0z}\tilde{u}_{0z}=\partial_z(\tilde{\mu}_{0z}(1+\tilde{u}_0))=0, \tag{3.12}$$

which implies $\tilde{\mu}_{0z}(1+\tilde{u}_0)=c_1$ in $(-\eta,\hat{\eta})$ and c_1 is a constant independent of z. For z in $[\hat{\eta},+\infty)$, we have

$$\tilde{\mu}_{0zz}(1+\tilde{u}_0)=0. \tag{3.13}$$

In this case, $\tilde{\mu}_0=a_1z+b_1$. Here a_1 and b_1 are some functions independent of z. However, we claim $a_1=0$ since $\tilde{\mu}_0$ must be bounded. This leads to $\tilde{\mu}_0=b_1$. Moreover, recall that

$$\tilde{\mu}_0=F'(\tilde{u}_0)-\partial_{zz}\tilde{u}_0,\quad \tilde{u}_0|_{x=\pm\infty}=\pm1. \tag{3.14}$$

We take the profile

$$\tilde{u}_0 = \tanh(z/\sqrt{2}), \quad \tilde{\mu}_0 = 0, \quad \forall z \in [\hat{\eta}, +\infty). \tag{3.15}$$

By the smooth continuity of $\tilde{\mu}_0$ at $\hat{\eta}$, we have $c_1 = 0$ and $\tilde{\mu}_0 = 0$ in $(-\eta, +\infty)$.

Now we consider the governing function of the front. The time-fractional derivative in this scaling is

(3.16)

$$\begin{aligned}
\partial_t^\alpha u(x,t) &= \partial_t^\alpha \big((\tilde{u}_0 + \varepsilon\tilde{u}_1 + \cdots)(\phi(x,t)/\varepsilon, x, t)\big) \\
&= \frac{1}{\Gamma(1-\alpha)} \int_0^t \frac{\varepsilon^{-1}\partial_\tau\phi(x,\tau)\partial_z\tilde{u}_0(\phi(x,\tau)/\varepsilon, x, \tau) + (\partial_\tau\tilde{u}_0(z,x,\tau)|_{z=\phi(x,\tau)/\varepsilon})}{(t-\tau)^\alpha} d\tau \\
&+ \frac{1}{\Gamma(1-\alpha)} \int_0^t \frac{\partial_\tau\phi(x,\tau)\partial_z\tilde{u}_1(\phi(x,\tau)/\varepsilon, x, \tau) + \varepsilon\partial_\tau\tilde{u}_1(z,x,\tau)|_{z=\phi(x,\tau)/\varepsilon}}{(t-\tau)^\alpha} d\tau + \cdots.
\end{aligned}$$

Matching the $O(1/\varepsilon)$ terms in (3.16) together with (3.4) yields the equation

$$\begin{aligned}
&\frac{1}{\Gamma(1-\alpha)} \int_0^t \frac{\partial_\tau\phi(x,\tau)\partial_z\tilde{u}_0(\phi(x,\tau)/\varepsilon)\chi_0}{(t-\tau)^\alpha} d\tau \\
=&(\tilde{u}_{0z}\hat{\chi}_1\varepsilon^{-1} + \tilde{u}_{1z})\tilde{\mu}_{0z} + \tilde{u}_{0z}\hat{\chi}_0\tilde{\mu}_{1z} + \chi_0\kappa(1+\tilde{u}_0)\tilde{\mu}_{0z} \\
&+ \chi_0(1+\tilde{u}_0)\tilde{\mu}_{1zz} + (\tilde{u}_1 + \chi_1\tilde{u}_0\varepsilon^{-1})\tilde{\mu}_{0zz} \\
=&\chi_0(1+\tilde{u}_0)\tilde{\mu}_{1zz} + \hat{\chi}_0\tilde{u}_{0z}\tilde{\mu}_{1z} \\
=&\chi_0\partial_z((1+\tilde{u}_0)\tilde{\mu}_{1z}) + (\hat{\chi}_0 - \chi_0)\tilde{u}_{0z}\tilde{\mu}_{1z},
\end{aligned} \tag{3.17}$$

which is simplified by using the former results (3.15). Integrating (3.17) over $(-\infty, \infty)$, we have

$$\partial_{t_1}^\alpha \phi\tilde{u}_0|_{-\eta}^{\hat{\eta}} = (1+\tilde{u}_0)\tilde{\mu}_{1z}|_{-\eta}^{+\infty} - \tilde{u}_{0z}\tilde{\mu}_{1z}|_{\hat{\eta}}^{+\infty}. \tag{3.18}$$

Here $-1 \le \tilde{u}_0(-\eta) \le -1 + O(\varepsilon)$ and $1 - O(\varepsilon) \le \tilde{u}_0(\hat{\eta}) \le 1$. In addition, since $\tilde{\mu}_{1z}^{+\infty} = 0$, we could derive

(3.19)

$$\partial_t^\alpha\phi(2+O(\varepsilon)) = 2\lim_{z\to+\infty}\tilde{\mu}_{1z} - (1+\tilde{u}_0)\tilde{\mu}_{1z}|_{-\eta} + \tilde{u}_{0z}\tilde{\mu}_{1z}|_{\hat{\eta}} = 2\lim_{z\to+\infty}\tilde{\mu}_{1z} + O(\varepsilon).$$

Therefore, using the matching conditions,

$$\partial_t^\alpha\phi(2+O(\varepsilon)) = 2\lim_{z\to+\infty}\tilde{\mu}_{1z} + O(\varepsilon) = 2\partial_{\mathbf{m}}\tilde{\mu}_0^+ + O(\varepsilon). \tag{3.20}$$

By letting $\varepsilon \to 0$, we derive the sharp interface condition:

$$\partial_t^\alpha\phi = \partial_{\mathbf{m}}\tilde{\mu}_0^+. \tag{3.21}$$

Sharp interface model in $t = O(1)$. Combining (3.9), (3.14), and (3.21), we derive the following sharp interface model:

$$\partial_t^\alpha u_0 = \nabla((1+u_0)\nabla\mu_0), \quad \mu_0 = F'(u_0), \qquad \text{in} \quad \Omega/\Gamma, \tag{3.22a}$$

$$u_0 = \pm 1 \quad \text{on} \quad \Gamma^\pm, \quad \mu_0 = 0, \qquad \text{on} \quad \Gamma, \tag{3.22b}$$

$$\mathrm{I}^{1-\alpha}V = \partial_{\mathbf{m}}\mu_0^+ \qquad \text{on} \quad \Gamma. \tag{3.22c}$$

3.2. The timescale $t_1 = \varepsilon^{\frac{1}{\alpha}} t$: A one-sided time-fractional MS model.

3.2.1. Outer expansion. The same as (3.9), by asymptotic matching, it yields

$$0 = \nabla((1+u_0)\nabla\mu_0), \tag{3.23a}$$

$$\partial_{t_1}^{\alpha} u_0 = \nabla((1+u_0)\nabla\mu_1 + u_1\nabla\mu_0), \tag{3.23b}$$

$$\partial_{t_1}^{\alpha} u_1 = \nabla((1+u_0)\nabla\mu_2 + u_1\nabla\mu_1 + u_2\nabla\mu_0). \tag{3.23c}$$

Here μ_0, μ_1, μ_2 are the same as shown before. The first equation implies a equilibrium state, so we take the following solution in the outer region:

$$u_0 = \begin{cases} +1 & \text{in} \quad \Omega^+, \\ -1 & \text{in} \quad \Omega^-. \end{cases} \tag{3.24}$$

3.2.2. Inner expansion. The same as (3.10), asymptotic matching leads to

$$0 = \tilde{u}_{0z}\tilde{\mu}_{0z} + \chi_0(1+\tilde{u}_0)\tilde{\mu}_{0zz}, \tag{3.25}$$

$$\begin{aligned} 0 =& (\tilde{u}_{0z}\hat{\chi}_1\varepsilon^{-1} + \tilde{u}_{1z})\tilde{\mu}_{0z} + \tilde{u}_{0z}\hat{\chi}_0\tilde{\mu}_{1z} + \chi_0\kappa(1+\tilde{u}_0)\tilde{\mu}_{0z} + \chi_0(1+\tilde{u}_0)\tilde{\mu}_{1zz} + \\ & (\tilde{u}_1 + \chi_1\tilde{u}_0\varepsilon^{-1})\tilde{\mu}_{0zz}. \end{aligned} \tag{3.26}$$

Now we solve (3.25)–(3.26) as follows. Equation (3.25) is

$$\chi_0\partial_z((1+\tilde{u}_0)\tilde{\mu}_{0z}) + \hat{\chi}_0(1+\tilde{u}_0)\tilde{\mu}_{0zz} = 0. \tag{3.27}$$

For $z \in (-\eta, \hat{\eta})$, (3.27) is

$$\tilde{\mu}_{0zz}(1+\tilde{u}_0) + \tilde{\mu}_{0z}\tilde{u}_{0z} = \partial_z(\tilde{\mu}_{0z}(1+\tilde{u}_0)) = 0, \tag{3.28}$$

and, for $z \in [\hat{\eta}, +\infty)$, it is

$$\tilde{\mu}_{0zz}(1+\tilde{u}_0) = 0. \tag{3.29}$$

As in section 3.1, (3.28)–(3.29) can be solved by the exact function

$$\tilde{u}_0 = \tanh(z/\sqrt{2}), \quad \tilde{\mu}_0 = 0. \tag{3.30}$$

Next, we intend to determine $\tilde{u}_1$ and $\tilde{\mu}_1$. Using (3.30), (3.26) is simplified into

$$\chi_0(1+\tilde{u}_0)\tilde{\mu}_{1zz} + \hat{\chi}_0\tilde{u}_{0z}\tilde{\mu}_{1z} = 0, \tag{3.31}$$

which implies that $\tilde{\mu}_1 = c_2$ for $z \in (\hat{\eta}, +\infty)$. We assume that $\tilde{\mu}_1 = c_2$ for all z. Here c_2 is some constant independent of z. Recall that

$$\tilde{\mu}_1 = -\tilde{u}_{1zz} - \kappa\tilde{u}_{0z} + F''(\tilde{u}_0)\tilde{u}_1. \tag{3.32}$$

Noticing that $F''(u_0)u_0' - \partial_{zz}u_0' = 0$, multiplying (3.32) by u_0', and integrating the resulting one over $(-\infty, +\infty)$, we have

$$\tilde{\mu}_1 = c_2 = -\kappa\frac{S}{[U]}, \tag{3.33}$$

where $S = \int_{-\infty}^{+\infty} \tilde{u}_0'(z)^2 dz$ and $[U] = \tilde{u}_0|_{-\infty}^{+\infty}$.

As for $\tilde{u}_1$, we use the idea which was presented in [11]. We find that $\tilde{u}_1 = \kappa\Phi_0 + \alpha\tilde{u}_0'$, where Φ_0 satisfies

$$-\Phi_{0zz} + F''(\tilde{u}_0)\Phi_0 = \tilde{u}_{0z} - \frac{S}{[U]}. \tag{3.34}$$

We impose $\tilde{u}_1(0) = 0$ to center the function. Thus, it is determined that

$$\tilde{u}_1 = \kappa\Phi = \kappa(\Phi_0 - \frac{\Phi_0(0)}{\tilde{u}_0'(0)}\tilde{u}_0'), \tag{3.35}$$

where $\Phi(\pm\infty) = -\frac{S}{[U]F''(\pm 1)}$.

Now we derive the equation of the front line. Matching with respect to series of ε, we get

$$\begin{aligned}
&\frac{1}{\Gamma(1-\alpha)}\int_0^{t_1}\frac{\partial_\tau\phi(x,\tau)\partial_z\tilde{u}_0(\phi(x,\tau)/\varepsilon)\chi_0}{(t_1-\tau)^\alpha}d\tau \\
=&\nabla_x\tilde{u}_0\nabla_x\tilde{\mu}_0 + ((\hat{\chi}_0\tilde{u}_{0z}\varepsilon^{-1} + \tilde{u}_{1z})\tilde{\mu}_{1z} + \hat{\chi}_0\tilde{u}_{0z}\tilde{\mu}_{2z} + (\hat{\chi}_2\tilde{u}_0\varepsilon^{-2} + \tilde{u}_{2z})\tilde{\mu}_{0z}) \\
&+ \chi_0(1+\tilde{u}_0)(\Delta_x\tilde{\mu}_0 + \kappa\tilde{\mu}_{1z} + \tilde{\mu}_{2zz})(\varepsilon^{-1}(1+\tilde{u}_0)\chi_1 + \tilde{u}_1)(\kappa\tilde{\mu}_{0z} + \tilde{\mu}_{1zz}) + \\
&+ (\varepsilon^{-2}(1+\tilde{u}_0)\chi_2 + \tilde{u}_2)\tilde{\mu}_{0zz},
\end{aligned} \tag{3.36}$$

which yields, by using the known functions $\tilde{u}_0, \tilde{\mu}_0, \tilde{u}_1, \tilde{\mu}_1$, that

$$\frac{1}{\Gamma(1-\alpha)}\int_0^{t_1}\frac{\varepsilon^{-1}\partial_\tau\phi(x,\tau)\partial_z\tilde{u}_0(\phi(x,\tau)/\varepsilon)\chi_0}{(t_1-\tau)^\alpha}d\tau = \hat{\chi}_0\tilde{u}_{0z}\tilde{\mu}_{2z} + \chi_0(1+\tilde{u}_0)\tilde{\mu}_{2zz}, \tag{3.37}$$

which gives, by integrating in$(-\infty,\infty)$ and using the matching condition, that

$$\partial_{t_1}^\alpha\phi = \lim_{z\to+\infty}\tilde{\mu}_{2z} = \partial_{\mathbf{m}}\mu_1^+. \tag{3.38}$$

Sharp interface model in $t_1 = \varepsilon^{\frac{1}{\alpha}}t$. It follows from (3.23b), (3.33), and (3.38) that the sharp interface model in this timescale is

$$\partial_{t_1}^\alpha u_0 = \Delta\mu_1 \qquad \text{in} \quad \Omega^+, \tag{3.39a}$$

$$\mu_1 = -\kappa\frac{S}{2} \qquad \text{on} \quad \Gamma, \tag{3.39b}$$

$$\mathrm{I}^{1-\alpha}V = \partial_{\mathbf{m}}\mu_1^+ \qquad \text{on} \quad \Gamma, \tag{3.39c}$$

u_0 is the sign function of ϕ, and $u_0 = \pm 1$ in $\Omega^\pm$. We call (3.39a)–(3.39c) the time-fractional MS model. The front motion is governed only by the phase parameter restricted in Ω^+.

3.3. The timescale $t_2 = \varepsilon^{\frac{2}{\alpha}}t$.

3.3.1. Outer expansion. In this case, by asymptotic matching, it yields

$$0 = \nabla((1+u_0)\nabla\mu_0), \tag{3.40a}$$

$$0 = \nabla((1+u_0)\nabla\mu_1 + u_1\nabla\mu_0), \tag{3.40b}$$

$$\partial_{t_2}^\alpha u_0 = \nabla((1+u_0)\nabla\mu_2 + u_1\nabla\mu_1 + u_2\nabla\mu_0). \tag{3.40c}$$

Let us solve (3.40a)–(3.40c). Equation (3.40a) implies an equilibrium state, so it is reasonable to take static solutions in Ω^+ and Ω^-,

$$u_0 = \begin{cases} +1 & \text{in} \quad \Omega^+, \\ -1 & \text{in} \quad \Omega^-, \end{cases} \tag{3.41}$$

which yields, together with (3.40b)–(3.40c), that the governing equations of μ_1 in $\Omega^-$and μ_2 in Ω^+ are

$$\nabla(\mu_1 \nabla \mu_1) = \partial_{t_2}^{\alpha} u_0 \qquad \text{in} \quad \Omega^-, \tag{3.42a}$$

$$\Delta \mu_1 = 0 \qquad \text{in} \quad \Omega^+, \tag{3.42b}$$

$$2\Delta \mu_2 + \frac{1}{2}\nabla(\mu_1 \nabla \mu_1) = \partial_{t_2}^{\alpha} u_0 \qquad \text{in} \quad \Omega^+. \tag{3.42c}$$

Therefore, we take the solution that μ_1 is a constant in Ω^+.

3.3.2. Inner expansion. Similarly, asymptotic matching ε yields

$$0 = \tilde{u}_{0z}\tilde{\mu}_{0z} + \chi_0(1+\tilde{u}_0)\tilde{\mu}_{0zz}, \tag{3.43}$$

$$\begin{aligned} 0 =& (\tilde{u}_{0z}\hat{\chi}_1\varepsilon^{-1} + \tilde{u}_{1z})\tilde{\mu}_{0z} + \tilde{u}_{0z}\hat{\chi}_0\mu_{1z} + \chi_0\kappa(1+\tilde{u}_0)\tilde{\mu}_{0z} + \chi_0(1+\tilde{u}_0)\tilde{\mu}_{1zz} \\ &+ (\tilde{u}_1 + \chi_1\tilde{u}_0\varepsilon^{-1})\tilde{\mu}_{0zz}, \end{aligned} \tag{3.44}$$

$$\begin{aligned} 0 =& \nabla_x\tilde{u}_0\nabla_x\tilde{\mu}_0 + ((\hat{\chi}_0\tilde{u}_{0z}\varepsilon^{-1} + \tilde{u}_{1z})\tilde{\mu}_{1z} + \hat{\chi}_0\tilde{u}_{0z}\tilde{\mu}_{2z} + (\hat{\chi}_2\tilde{u}_0\varepsilon^{-2} + \tilde{u}_{2z})\tilde{\mu}_{0z}) \\ &+ \chi_0(1+\tilde{u}_0)(\Delta_x\tilde{\mu}_0 + \kappa\tilde{\mu}_{1z} + \tilde{\mu}_{2zz}) + (\varepsilon^{-1}(1+\tilde{u}_0)\chi_1 + \tilde{u}_1)(\kappa\tilde{\mu}_{0z} + \tilde{\mu}_{1zz}) \\ &+ (\varepsilon^{-2}(1+\tilde{u}_0)\chi_2 + \tilde{u}_2)\tilde{\mu}_{0zz}, \end{aligned} \tag{3.45}$$

and

$$\begin{aligned} &\frac{1}{\Gamma(1-\alpha)}\int_0^{t_2} \frac{\partial_\tau\phi(x,\tau)\partial_z\tilde{u}_0(\phi(x,\tau)/\varepsilon)\chi_0}{(t_2-\tau)^\alpha}d\tau \\ =& \nabla_x\tilde{u}_0\nabla_x\tilde{\mu}_1 + \nabla_x\tilde{u}_1\nabla_x\tilde{\mu}_0 + (\hat{\chi}_0\tilde{u}_{0z}\tilde{\mu}_{3z} + (\hat{\chi}_1\tilde{u}_{0z}\varepsilon^{-1} + \tilde{u}_{1z})\tilde{\mu}_{2z} \\ &+ (\hat{\chi}_2\tilde{u}_{0z}\varepsilon^{-2} + \tilde{u}_{2z})\tilde{\mu}_{1z} + (\hat{\chi}_3\tilde{u}_{0z}\varepsilon^{-3} + \tilde{u}_{3z})\tilde{\mu}_{0z}) \\ &+ \chi_0(1+\tilde{u}_0)(\Delta_x\tilde{\mu}_1 + \kappa\tilde{\mu}_{2z} + \tilde{\mu}_{3zz}) \\ &+ ((1+\tilde{u}_0)\chi_1\varepsilon^{-1} + \tilde{u}_1)(\Delta_x\tilde{\mu}_0 + \kappa\tilde{\mu}_{0z} + \tilde{\mu}_{2zz}) \\ &+ ((1+\tilde{u}_0)\chi_2\varepsilon^{-2} + \tilde{u}_2)(\kappa\tilde{\mu}_{0z} + \tilde{\mu}_{1zz}) + ((1+\tilde{u}_0)\chi_3\varepsilon^{-3} + \tilde{u}_3)\tilde{\mu}_{0zz}, \end{aligned} \tag{3.46}$$

where the solutions of the first and the second equations, following the same treatment as in former sections, derive

$$\tilde{u}_0 = \tanh(z/\sqrt{2}), \quad \tilde{\mu}_0 = 0, \quad \tilde{\mu}_1 = \kappa S/2, \quad \tilde{u}_1 = \kappa\Phi. \tag{3.47}$$

As for $\tilde{\mu}_2$, we simplify (3.45) by (3.47) to derive

$$0 = \hat{\chi}_0\tilde{u}_{0z}\mu_{2z} + \chi_0(1+\tilde{u}_0)\tilde{\mu}_{2zz}, \tag{3.48}$$

which leads to $\tilde{\mu}_2 = b_2$ in $(-\eta, +\infty)$, where b_2 is a constant independent of z. Recall that by asymptotic matching,

$$\mu_2 = F''(\tilde{u}_0)\tilde{u}_2 - \tilde{u}_{2zz} - \kappa\tilde{u}_{1z} + F'''(\tilde{u}_0)\tilde{u}_1^2/2. \tag{3.49}$$

Multiplying (3.49) by $\tilde{u}_0'$ and integrating the resulting one over $(-\infty, +\infty)$, we get

$$\tilde{\mu}_2 \tilde{u}_0|_{-\infty}^{+\infty} = -\kappa^2 \int_{-\infty}^{+\infty} (\Phi' - \frac{1}{2} F'''(\tilde{u}_0)\Phi^2) u_{0z} dz \tag{3.50}$$

in $(\hat{\eta}, +\infty)$, which is

$$\tilde{\mu}_2 = -\kappa^2 S_1/2 \tag{3.51}$$

if we let $S_1 = \kappa^2 \int_{-\infty}^{+\infty} (\Phi' - \frac{1}{2} F'''(\tilde{u}_0)\Phi^2) u_{0z} dz$. Then, as in [11], we extrapolate a little bit, and one may assume that $\tilde{\mu}_2 = -\kappa^2 S_1/2$ in $(-\eta, \hat{\eta})$.

Now we solve for $\partial_t^\alpha \phi$. Using (3.47), we have

$$\begin{aligned} &\frac{1}{\Gamma(1-\alpha)} \int_0^{t_2} \frac{\partial_\tau \phi(x,\tau) \partial_z \tilde{u}_0(\phi(x,\tau)/\varepsilon)\chi_0}{(t_2-\tau)^\alpha} d\tau \\ =&\tilde{u}_{1z}\tilde{\mu}_{2z} + \tilde{u}_1 \tilde{\mu}_{2zz}\chi_0 (1+\tilde{u}_0)\tilde{\mu}_{3zz} + \hat{\chi}_0 \tilde{u}_{0z}\tilde{\mu}_{3z} \\ =&\chi_0 \partial_z((1+\tilde{u}_0)\tilde{\mu}_{3z}) - (\chi_0 - \hat{\chi}_0)\tilde{u}_{0z}\tilde{\mu}_{3z} + \partial_z(\tilde{u}_1 \tilde{\mu}_{2z}), \end{aligned} \tag{3.52}$$

which yields, by integrating over $(-\infty, +\infty)$, that

$$\partial_{t_2}^\alpha \phi(2+O(\varepsilon)) = \lim_{-\eta \to -\infty} ((1+\tilde{u}_0)\tilde{\mu}_{3z}) + 2\partial_{\mathbf{m}} \mu_2^+ + \lim_{-\eta \to -\infty} (\tilde{u}_1 \tilde{\mu}_{2z}) - \lim_{\hat{\eta} \to +\infty} u_{0z}\tilde{\mu}_{3z} + O(\varepsilon). \tag{3.53}$$

Using the matching conditions and letting $\varepsilon \to 0$, we get

$$2\partial_{t_2}^\alpha \phi = 2\partial_{\mathbf{m}} \mu_2^+ + u_1^- \partial_{\mathbf{m}} \mu_1^-, \tag{3.54}$$

which gives, by using $\mu_1 = F''(u_0)u_1 = 2u_1$, that

$$\partial_{t_2}^\alpha \phi = \partial_{\mathbf{m}} \mu_2^+ + \frac{1}{4} \mu_1^- \partial_{\mathbf{m}} \mu_1^-. \tag{3.55}$$

Sharp interface model at $t_2 = \varepsilon^{\frac{2}{\alpha}} t$. Combining (3.42a) and (3.42c) with (3.47), (3.51), and (3.55), we finally derive the sharp interface model in this timescale,

$$\nabla(\mu_1 \nabla \mu_1) = \partial_{t_2}^\alpha u_0 \qquad \text{in} \quad \Omega^-, \tag{3.56a}$$

$$\mu_1 = -\kappa \frac{S}{[U]} \qquad \text{on} \quad \Gamma, \tag{3.56b}$$

$$2\Delta \mu_2 = \partial_{t_2}^\alpha u_0 \qquad \text{in} \quad \Omega^+, \tag{3.56c}$$

$$\mu_2 = -\kappa^2 \frac{S_1}{[U]} \qquad \text{on} \quad \Gamma, \tag{3.56d}$$

$$\mathrm{I}^{1-\alpha} V = \partial_{\mathbf{m}} \mu_2^+ + \frac{1}{4} \mu_1^- \partial_{\mathbf{m}} \mu_1^- \qquad \text{on} \quad \Gamma, \tag{3.56e}$$

where u_0 is the sign function of ϕ, i.e., $u_0 = \pm 1$ in $\Omega^\pm$.

4. Scaling invariant property and coarsening rate heuristic. In physics, coarsening is a progcess when the pattern formed by the material "coarsens" and during which the "typical length scale" of the system is increasing. For phase-field models, since the energy of the system is proportional to the area of the interfacial layer, energy decay would result in the reduction of the interface layer, and the pattern

coarsens. Coarsening phenomena are also observed in numerical simulations of the pattern formation governed by TFCHE. As many people believe, coarsening is due to some "scaling invariant" property of the system, so the scaling invariant power law of the sharp interface model coincides in the coarsening rate in the simulation of [11, 22, 29].

Consider the nonlocal MS model with constant mobility in the $t_1 = \varepsilon^{\frac{1}{\alpha}} t$ timescale. It is scaling invariant in the following sense. Rescalen μ, x, t, and ϕ by

$$x = X\hat{x}, \quad t = T\hat{t}, \quad \mu = M\hat{\mu}, \quad \phi(x,t) = X\hat{\phi}(\hat{x},\hat{t}).$$

Direct calculation leads to

$$\kappa = X^{-1}\hat{\kappa}, \quad \partial_t^\alpha \phi = X/T^\alpha \partial_{\hat{t}}^\alpha \hat{\phi}, \quad \partial_{\mathbf{m}}\mu = X^{-2}\partial_{\hat{m}}\hat{\mu},$$

and

$$\frac{M}{X^2}\hat{\Delta}\hat{\mu} = \frac{1}{T^\alpha}\partial_{\hat{t}}^\alpha \hat{u}_0 \qquad \text{in} \quad \Omega\backslash\Gamma, \tag{4.1a}$$

$$M\hat{\mu} = \frac{1}{X}\hat{\kappa}\frac{S}{[U]} \qquad \text{on} \quad \Gamma, \tag{4.1b}$$

$$\frac{X}{T^\alpha}\partial_{\hat{t}}^\alpha \hat{\phi} = \frac{M}{X}[\partial_{\hat{m}}\hat{\mu}]_-^+[U]^{-1} \qquad \text{on} \quad \Gamma. \tag{4.1c}$$

If taking $M = X^{-1}$ and $T^\alpha = X^3$, the system has exactly the same form as (2.35a)–(2.35d). This is the scaling invariance property and it shows that the typical length scale l of this model satisfies an $l \sim ct^{\frac{\alpha}{3}}$ power law, which implies that the TFCHE admits a coarsening rate of $\frac{\alpha}{3}$. This result fits the numerical experiments in [34, 38] well.

In the second part of this section, we aim to use this idea to determine the coarsening rate of the sharp interface models of the degenerate TFCHE. First, for the sharp interface models in the $t_1 = \varepsilon^{\frac{1}{\alpha}} t$ timescale,

$$\partial_{t_1}^\alpha u_0 = \Delta\mu_1 \qquad \text{in} \quad \Omega^+, \tag{4.2a}$$

$$\mu_1 = -\kappa\frac{S}{[U]} \qquad \text{on} \quad \Gamma, \tag{4.2b}$$

$$\mathrm{I}^{1-\alpha} V = \partial_{\mathbf{m}}\mu_1^+ \qquad \text{on} \quad \Gamma, \tag{4.2c}$$

by using the same rescaling as in (4.1c)–(4.1a),

$$x = \lambda^{\frac{\alpha}{3}}\hat{x}, \quad t_1 = \lambda\hat{t}_1, \quad \mu_1 = \lambda^{-\frac{\alpha}{3}}\hat{\mu}_1, \quad \phi(x,t_1) = \lambda^{\frac{\alpha}{3}}\hat{\phi}(\hat{x},\hat{t}_1),$$

we find that (4.2a)–(4.2c) preserves a $\frac{\alpha}{3}$ coarsening rate, too.

On the other hand, for the sharp interface model (1.8a)–(1.8e) in the $t_2 = \varepsilon^{\frac{2}{\alpha}} t$ timescale,

$$\partial_{t_2}^\alpha u_0 = \nabla(\mu_1\nabla\mu_1) \qquad \text{in} \quad \Omega^-, \tag{4.3a}$$

$$\mu_1 = -\kappa\frac{S}{[U]} \qquad \text{on} \quad \Gamma, \tag{4.3b}$$

$$\partial_{t_2}^\alpha u_0 = 2\Delta\mu_2 \qquad \text{in} \quad \Omega^+, \tag{4.3c}$$

$$\mu_2 = -\kappa^2\frac{S_1}{[U]} \qquad \text{on} \quad \Gamma, \tag{4.3d}$$

$$\mathrm{I}^{1-\alpha} V = \partial_{\mathbf{m}}\mu_2^+ + \frac{1}{4}\mu_1^-\partial_{\mathbf{m}}\mu_1^- \qquad \text{on} \quad \Gamma. \tag{4.3e}$$

Taking M_1, M_2, T, X to be the length scales of the chemical potentials, time, and space, respectively, we rescale the above system (4.3a)–(4.3e) so that

$$\frac{1}{T^\alpha}\partial_{\hat{t}}^\alpha u_0 = \frac{M_1^2}{X^2}\nabla(\hat{\mu}_1\nabla\hat{\mu}_1) \qquad \text{in} \quad \Omega^-, \tag{4.4a}$$

$$M_1\hat{\mu}_1 = -\frac{1}{X}\hat{\kappa}\frac{S}{[U]} \qquad \text{on} \quad \Gamma, \tag{4.4b}$$

$$\frac{1}{T^\alpha}\partial_{\hat{t}}^\alpha u_0 = 2\frac{M_2}{X^2}\hat{\Delta}\hat{\mu}_2 \qquad \text{in} \quad \Omega^+, \tag{4.4c}$$

$$M_2\hat{\mu}_2 = -\frac{1}{X^2}\hat{\kappa}^2\frac{S_1}{[U]} \qquad \text{on} \quad \Gamma, \tag{4.4d}$$

$$\frac{X}{T^\alpha}\partial_{\hat{t}}^\alpha \mathrm{I}^{1-\alpha}\hat{V} = \frac{M_2}{X}\partial_{\mathbf{m}}\hat{\mu}_2^+ + \frac{M_1^2}{X}\frac{1}{4}\hat{\mu}_1^-\partial_{\mathbf{m}}\hat{\mu}_1^- \qquad \text{on} \quad \Gamma. \tag{4.4e}$$

The system is the same form as (1.8a)–(1.8e) if we take

$$T^\alpha = X^4, \quad M_1 = \frac{1}{X}, \quad \text{and} \quad M_2 = \frac{1}{X^2}.$$

It exhibits a power law relation $l \sim ct^{\frac{\alpha}{4}}$. Moreover, this power law indicate a coarsening rate of $\frac{\alpha}{4}$.

5. Discussion and conclusions. We study the front motion and obtain the corresponding sharp interface models of the TFCHE with two different kinds of diffusion mobilities. We find that in both cases, the sharp interface limits are sensitive to the timescale. For example, in a slow timescale $\varepsilon^{\frac{1}{\alpha}}t$, the asymptotic limits are fractional MS models, which are formally similar to classical MS models excepte for the nonlocal term.

Moreover, powerlaw arguments show that the nonlocal fractional MS model of TFCHE with constant mobility fits the $\frac{\alpha}{3}$ coarsening rate obtained in existing numerical experiments [38, 34]. Moreover, TFCHE with the one-sided degenerate mobility contains two stages of different coarsening rates $\frac{\alpha}{3}$ and $\frac{\alpha}{4}$. The results show that the TFCHE could be used to model the coarsening process with a general coarsening rate. We expect to extend similar arguments to the nonlocal-in-time phase-field equations, in which the time fractional operator is replaced by a nonlocal-in-time operator [16].

In this paper, we only study the TFCH asymptotically. The convergence analysis of TFCH to the sharp interface model is a challenging work due to the nonlocal effect of the fractional operator and the low regularity of the solution. Another interesting question is how to model the coarsening process with a rate greater than 1/3. Since our analysis suggests that TFCHE with constant mobility admits a coarsening rate $\alpha/3$ and it contains two stages of different coarsening rates $\frac{\alpha}{3}$ and $\frac{\alpha}{4}$ for the one-sided degenerate mobility, one possible way is to find proper mobilities.

REFERENCES

[1] N. D. Alikakos, P. W. Bates, and X. Chen, *Convergence of the Cahn–Hilliard equation to the Hele–Shaw model*, Arch. Ration. Mech. Anal., 128 (1994), pp. 165–205.

[2] M. Allen, L. Caffarelli, and A. Vasseur, *A parabolic problem with a fractional time derivative*, Arch. Ration. Mech. Anal., 221 (2016), pp. 603–630.

[3] F. Bernis and A. Friedman, *Higher order nonlinear degenerate parabolic equations*, J. of Differential Equations, 83 (1990), pp. 179–206.

[4] L. A. Caffarelli and N. E. Muler, *An L^∞ bound for solutions of the Cahn–Hilliard equation*, Arch. Ration. Mech. Anal., 133 (1995), pp. 129–144.

[5] G. Caginalp and P. C. Fife, *Dynamics of layered interfaces arising from phase boundaries*, SIAM J. Appl. Math., 48 (1988), pp. 506–518.
[6] J. W. Cahn, C. M. Elliott, and A. Novick-Cohen, *The Cahn–Hilliard equation with a concentration dependent mobility: Motion by minus the Laplacian of the mean curvature*, Eur. J. Appl. Math., 7 (1996), pp. 287–301.
[7] Z. Cai, C. Zhang, R. Wang, C. Peng, K. Qiu, and N. Wang, *Effect of solidification rate on the coarsening behavior of precipitate in rapidly solidified Al-Si alloy*, Prog. in Nat. Sci. Mater. Int., 26 (2016), pp. 391–397.
[8] L. Chen, J. Zhang, J. Zhao, W. Cao, H. Wang, and J. Zhang, *An accurate and efficient algorithm for the time-fractional molecular beam epitaxy model with slope selection*, Comput. Phys. Commun., 245 (2019), 106842.
[9] W. Chen, S. Conde, C. Wang, X. Wang, and S. M. Wise, *A linear energy stable scheme for a thin film model without slope selection*, J. Sci. Comput., 52 (2012), pp. 546–562.
[10] L. F. Cugliandolo, *Coarsening phenomena*, C. R. Phys., 16 (2015), pp. 257–266.
[11] S. Dai and Q. Du, *Motion of interfaces governed by the Cahn–Hilliard equation with highly disparate diffusion mobility*, SIAM J. Appl. Math., 72 (2012), pp. 1818–1841.
[12] S. Dai and Q. Du, *Computational studies of coarsening rates for the Cahn–Hilliard equation with phase-dependent diffusion mobility*, J. Comput. Phys., 310 (2016), pp. 85–108.
[13] S. Dai, B. Niethammer, and R. L. Pego, *Crossover in coarsening rates for the monopole approximation of the Mullins–Sekerka model with kinetic drag*, Proc. Roy. Soc. Edinburgh Sect. A, 140 (2010), pp. 553–571.
[14] S. Dai and R. L. Pego, *Universal bounds on coarsening rates for mean-field models of phase transitions*, SIAM J. Math. Anal., 37 (2005), pp. 347–371.
[15] Q. Du and J. Yang, *Asymptotically compatible Fourier spectral approximations of nonlocal Allen–Cahn equations*, SIAM J. Numer. Anal., 54 (2016), pp. 1899–1919.
[16] Q. Du, J. Yang, and Z. Zhou, *Analysis of a nonlocal-in-time parabolic equation*, Discrete Contin. Dyn. Syst.-B, 22 (2017), 339.
[17] Q. Du, J. Yang, and Z. Zhou, *Time-fractional Allen–Cahn equations: Analysis and numerical methods*, J. Sci. Comput., 85 (2020), pp. 1–30.
[18] M. Dziwnik, A. Münch, and B. Wagner, *An anisotropic phase-field model for solid-state dewetting and its sharp-interface limit*, Nonlinearity, 30 (2017), 1465.
[19] C. Garay-Reyes, S. Hernández-Martínez, J. Hernández-Rivera, J. Cruz-Rivera, E. Gutiérrez-Castañeda, H. Dorantes-Rosales, J. Aguilar-Santillan, and R. Martínez-Sánchez, *Comparative study of Oswald ripening and trans-interface diffusion-controlled theory models: Coarsening of γ' precipitates affected by elastic strain along a concentration gradient*, Metals Mater. Int., 23 (2017), pp. 298–307.
[20] S. Jiang, J. Zhang, Q. Zhang, and Z. Zhang, *Fast Evaluation of the Caputo Fractional Derivative and Its Applications to Fractional Diffusion Equations*, preprint, arXiv:1511.03453, 2015.
[21] A. A. Kilbas, H. M. Srivastava, and J. J. Trujillo, *Theory and Applications of Fractional Differential Equations*, Vol. 204, Elsevier, Amstardam, 2006.
[22] R. V. Kohn and X. Yan, *Coarsening rates for models of multicomponent phase separation*, Interfaces Free Bound., 6 (2004), pp. 135–149.
[23] K. N. Le, W. McLean, and K. Mustapha, *Numerical solution of the time-fractional Fokker–Planck equation with general forcing*, SIAM J. Numer. Anal., 54 (2016), pp. 1763–1784.
[24] Z. Li, H. Wang, and D. Yang, *A space-time fractional phase-field model with tunable sharpness and decay behavior and its efficient numerical simulation*, J. Comput. Phys., 347 (2017), pp. 20–38.
[25] Y. Lin and C. Xu, *Finite difference/spectral approximations for the time-fractional diffusion equation*, J. Comput. Phys., 225 (2007), pp. 1533–1552.
[26] H. Liu, A. Cheng, H. Wang, and J. Zhao, *Time-fractional Allen–Cahn and Cahn–Hilliard phase-field models and their numerical investigation*, Comput. Math. Appl., 76 (2018), pp. 1876–1892.
[27] H. Liu, A. Cheng, H. Wang, and J. Zhao, *Time-fractional Allen–Cahn and Cahn–Hilliard phase-field models and their numerical investigation*, Comput. Math. Appl., 76 (2018), pp. 1876–1892.
[28] R. L. Pego, *Front migration in the nonlinear Cahn–Hilliard equation*, Proc. Roy. Soc. Lond. A, 422 (1989), pp. 261–278.
[29] R. L. Pego, *Lectures on dynamics in models of coarsening and coagulation*, in Dynamics in Models of Coarsening, Coagulation, Condensation and Quantization, Vol. 9, World Scientific, Singapore, 2007, pp. 1–61.

[30] I. Podlubny, *Fractional Differential Equations: An Introduction to Fractional Derivatives, Fractional Differential Equations, to Methods of Their Solution and Some of Their Applications*, Elsevier, Amsterdam, 1998.
[31] S. G. Samko, A. A. Kilbas, and O. I. Marichev, *Fractional Integrals and Derivatives*, vol. 1, Gordon and Breach Science Publishers, Yverdon, Switzerland, 1993.
[32] A. Sequeira, H. Calderon, G. Kostorz, and J. Pedersen, *Bimodal size distributions of γ' precipitates in Ni-Al-Mo*—ii. *Transmission electron microscopy*, Acta Metallurgica Mater., 43 (1995), pp. 3441–3451.
[33] J. Shen and X. Yang, *Numerical approximations of Allen–Cahn and Cahn–Hilliard equations*, Discrete Contin. Dyn. Syst., 28 (2010), pp. 1669–1691.
[34] T. Tang, H. Yu, and T. Zhou, *On energy dissipation theory and numerical stability for time-fractional phase-field equations*, SIAM J. Sci. Comput., 41 (2019), pp. A3757–A3778.
[35] Y. Yan, W. Chen, C. Wang, and S. M. Wise, *A second-order energy stable BDF numerical scheme for the Cahn-Hilliard equation*, Commun. Comput. Phys., 23 (2018), pp. 572–602.
[36] J. Yin, *On the existence of nonnegative continuous solutions of the Cahn–Hilliard equation*, J. Differential Equations, 97 (1992), pp. 310–327.
[37] J. Zhang, J. Zhao, and J. Wang, *A non-uniform time-stepping convex splitting scheme for the time-fractional Cahn–Hilliard equation*, Comput. Math. Appl., 80 (2020), pp. 837–850.
[38] J. Zhao, L. Chen, and H. Wang, *On power law scaling dynamics for time-fractional phase field models during coarsening*, Commun. Nonlinear Sci. Numer. Simul., 70 (2019), pp. 257–270.